Effects of Line Defect on Electronic Transport of Double Gate Armchair Graphene Nanoribbon Field Effect Transistors: a Simulation Study

Mohammad Bagher Nasrollahnejad^{1*}, Parviz Keshavarzi^{2}

Abstract – Defect engineering in nonmaterials could be used to modify the properties of materials for various practical applications. In this paper, the impact of linear arrangement of ISTW (LA-ISTW) defect and its position on the transport properties of grapheme nanoribbon transistors is investigated. The analysis show that creating the LA-ISTW defect with a certain density in the proper position of the channel length leads to increase the bandgap, suppress ambipolar conduction and provides the higher on-off current ratio and therefore the structure with LA-ISTW defect in the proper defect position and the specified defect density has better performance than conventional structure. The results have also demonstrated the defect engineering potential on modifying the electronic transport properties of GNR FETs. Simulations has been done based on self-consistent solution of full 3D Poisson and Schrodinger equations within the non-equilibrium Green's function formalism. Graphene nanoribbons with non-passivated edges are used in the transistor channel.

Keywords: Inverse Stone Thrower Wales defect; Electronic transport properties; Graphene nanoribbon field-effect transistor; Non-equilibrium Green's function formalism.

.

1. Introduction

Graphene known as a 2D semi-metallic material arranged in honeycomb lattice structure [1]. Its excellent properties such as high carrier mobility [2], superior thermal [3] and electrical conductivity have led to progress of GNR based devices [4]. So graphene is an appropriate material for achieving future generation transistors with high efficiency and speed. Despite these advantages, strong ambipolarity effect and lack of band gap in graphene structures led to some challenges in digital electronic applications [5-6]. To get better electronic transport properties of the graphene, the graphene lattice structures have to be changed. Introducing the topological defects can also change the intrinsic gap of graphene and consequently improve electronic transport properties of the graphene nanoribbon (GNR) devices [7-15].

There are various types of structural defects in graphene sheets, such as adatoms, vacancies, Stone-Wales (SW) and inverse Stone Throwers Wales (ISTW) [16-24].

Inverse Stone Thrower Wales (ISTW) defect which predicted earlier as a defect on graphene by Lusk et al. [25], is formed by adding two extra carbon atoms to 6-ring (see Figure 1 (a) [26]. ISTW defects can be produced by means of microscope electron, ion irradiation and chemical methods [7, 27]. There are few investigations about the impact of ISTW defect on graphene structures [25-26, 28-29]. Fotoohi et al. [28-29] investigated electronic and transport properties of zigzag and armchair graphene nanoribbons in a two terminal structure in presence of ISTW defect. We also submitted a paper which in the symmetry and position impact of ISTW defect on transport properties of DG-GNRFETs was investigated [30]. These investigations confirm the possibility of developing ISTW defects on graphene layer and therefore the possibility of defect engineering.

Defects can also be linearly aligned to create extended line defects (ELDs). Extended line defects can be effective to direct charge transport in graphene structures [31-36]. Magnetic properties of graphene with "5-5-8" line defect were investigated by Kou et al. [31]. They realized a ground state with weak ferromagnetic behavior and spin-

---

1* **Corresponding Author :** Department of Electrical Engineering, Gorgan Branch, Islamic Azad University, Gorgan, Iran. Email: M.Nasrollahnejad@gorganiau.ac.ir

2 Electrical and Computer Engineering Department, Semnan University, Semnan, Iran

Received 2020.03.15 ; Accepted 2020.06.24

polarized carriers localized along the line defect. Chen et al. explained the production method of extremely regular “5-5-8” line defects in graphene sheets [33]. They indicated an intense energy dependence on valley transport properties, which can be applied in switching nanodevices. Recently, a particular extended line defects (ELD) was reported by Lahiri et al [34]. By applying Stone Wales defect and deviancies in graphene sheets, they created 5-8-5 line defects. They concluded which 1D line defect can be applied as metallic wire. In the following, a valley filter was offered based on extended line defect by Gunlycke et al [36]. Bahamon et al. [37] observed Fabry-Perot oscillation and metallic characteristics in graphene line defects. However, effect of LA-ISTW defect on electronic characteristics of graphene transistors has not been studied, yet.

In this paper, for the first time, effect of locating LA-ISTW defect in various positions of length of channel of DG-AGNREFT is investigated. Figure1 depicts ISTW and LA-ISTW defects along the AGNR channel. It is shown that using LA-ISTW defect in an appropriate position along the channel leads to increase of energy gap, reduction of ambipolar behavior and increase of the on/off current ratio. Consequently, this defect improves transistor performance. In this paper, at first, computational methods applied in simulations and device configuration is considered and then simulation results for the structure presented is investigated. It is also shown that LA-ISTW defects influence on electron transport in DG-AGNRFETs and finally simulation results is discussed.

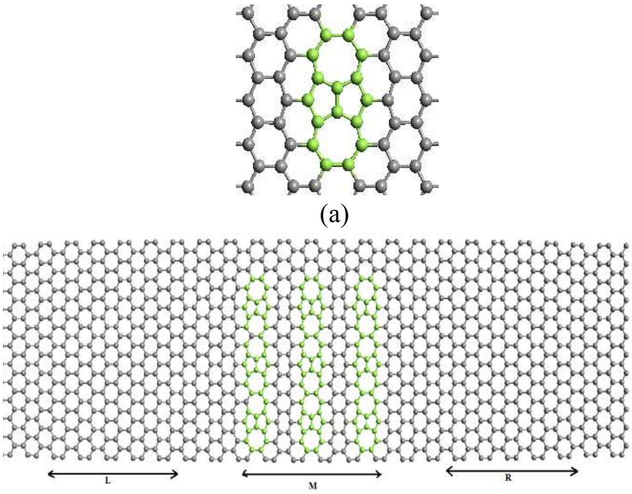

(a)

(b)

Figure 1: (a) ISTW defect and (b) three parallel linear arrangements of ISTW defects in channel length.

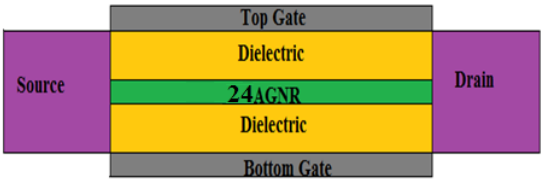

Figure 2: Schematic diagram of a DG- AGNR-FET device.

2. Device configuration and computational method

The schematic diagram of a DG-AGNRFET [38-39] is shown in Figure 2. AGNR is used as channel; contacts are made by extensions of AGNR channel. The length and width of channel material are 10nm and 1.35nm, respectively. The width of the channel material is composed of 24 atoms which are located between the top and bottom dielectric layers. The dielectric thickness is 3nm and its constant is 3.9ε0 which is close to silicon dioxide (sio2) dielectric constant. All of the transport calculations are performed using fully self-consistent tight binding model which is combined with nonequilibrium Green function formalism (NEGF) [40-41]. The retarded Green's function (GD) is computed as follows:

$$G_D = [(E + i\eta)I - H_T - U - \textstyle\sum_s - \sum_d]^{-1} \qquad (1)$$

In which ∑s and ∑d are the self-energie matrices of source and drain region, respectively; HT is the tight-binding Hamiltonian matrix of the AGNR channel; U is the electrostatic potential; and η is infinitesimally small quantity. Poisson equation shows electrostatic potential distribution across the channel. Transports equations represent the charge transport between drain and source regions. Electrostatic potential U is obtained by solving the Poisson equation under Dirichlet boundary condition along the transport direction and Neumann boundary condition in other boundaries. Poisson equation is as follows:

$$\nabla^2 U = -\frac{q}{\varepsilon}\rho \qquad (2)$$

Where ε is dielectric constant and ρ is charge density that calculated by solving Schrodinger equation using the NEGF formalism.

Transmission coefficient can be expressed as:

$$T(E) = \mathrm{Trace}[\Gamma_s G_D^r \Gamma_d G_D^a], \qquad (3)$$

Where □s/d=i(∑s/d-∑s/d†) is coupling between contacts and device; GrD and GaD show retarded and advanced Green's functions.

Electrical current is calculated though transmission spectrum applying Landauer-Butiker equation [41]:

$$I = \frac{q}{h}\int_{-\infty}^{+\infty} T(E)\left[f\left(E-\mu_S\right)-f\left(E-\mu_D\right)\right]dE, \qquad (4)$$

Where T(E) is probability of passing of carriers with energy E through channel, q is carrier charge, h is Planck constant and f(E-μS(D)) is Fermi-Dirac distribution of carriers in contacts in chemical potential μS(D). All geometric nanostructures become relaxed so that atomic forces can't exceed 0.001eV/Å and calculations are carried out at temperature T=300 K. Defects of LA-ISTW are distributed parallel across the channel length in three different positions of mid-channel, near the source and drain contacts.

3. Results and discussions

In this section, the effect of LA-ISTW defect on transport properties of DG-AGNRFET is investigated. Defects are considered in three positions: mid-channel, near the source and drain.

The carriers transport behavior is very important when the carriers travel throughout the AGNR channel. Therefore, the local density of states (LDOS) profile is depicted for the conventional and the defected structures (Figures 3, 4). The impact of ISTW defect on bandgap increasing is well illustrated in LDOS profiles. To evaluate the role of defect density in increasing the bandgap, three different defect densities of 0.5, 1 and 1.5 percent in three different positions of the channel length are considered. In this paper, defect densities are defined as the density of atoms added to the pristine AGNR channel [42]. Figure 3 depicts LDOS profile for the conventional structure and the structures with LA-ISTW defects in the left side of the channel. As shown in Figure 3, increasing the defect density from 0 to 1.5 % led to increases the bandgap from 0.5 to 0.75 eV. Figure 4 depicts LDOS profile for structures with LA-ISTW defects in the center and the right side of the channel in three different defect densities. The 1.5% defects density at the center significantly increases the bandgap up to 0.87eV. So the 1.5% defect densities are used as the best results for the rest of simulations. Although the results also show that only increasing the defect densities near drain contact has no considerable impact on bandgap.

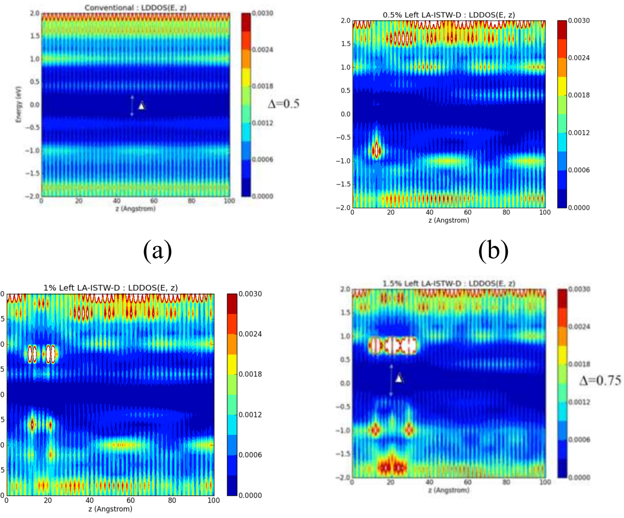

(a) (b)

(c) (d)

Figure 3: LDOS for (a) the C-AGNRFET and DG-AGNRFET with LA-ISTW defect in the left position of the channel for the three defect densities of (b) 0.5%, (c) 1% and (d) 1.5%. (VGS=0,VDS=0). In the white regions, the LDOSs are very high and those decrease as the regions become darker.

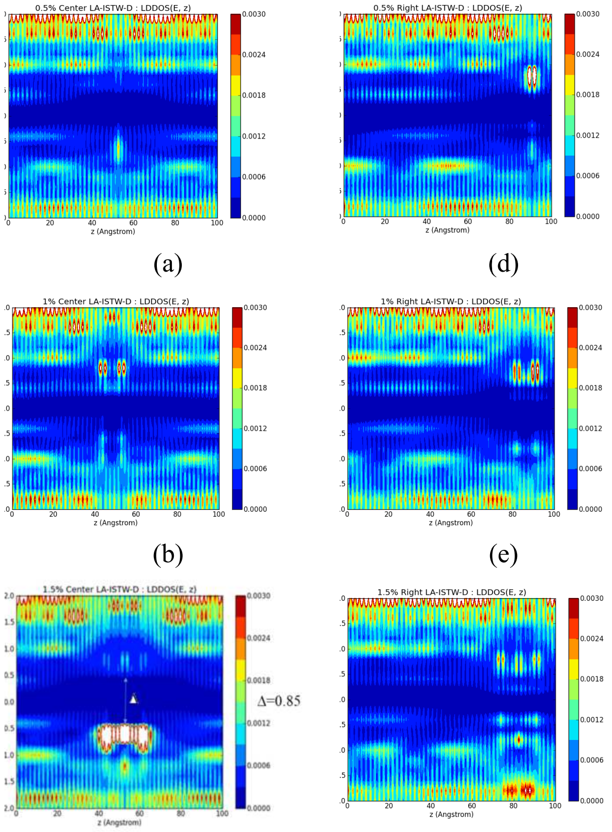

(a) (d)

(b) (e)

(c) (f)

Figure 4: LDOS for DG-AGNRFET with LA-ISTW defect in the center and right position of the channel for the three defect densities of (a,d) 0.5%, (b,e) 1% and (c,f) 1.5%.(VGS=0,VDS=0).

Adding such defects to the center of the channel length creates a big potential barrier in carrier transmission direction and leads to drop the transistor current. Figure 3 and Figure 4 also show that the regions with defect along the channel create localized states which trap carriers in transport direction. These states produce elastic scattering centers and reduce near-ballistic transport along the channel [11]. However, the bandgap increasing due to the defects is local and this bandgap only increases in the defective regions. Therefore, to investigate effects of defects on transport properties across the channel length, transmission spectrum is also used.

Transmission spectrum for the conventional structure and the structures with defect were drawn in Figure 5. The results show that the transport gap [43] of conventional, left, center and right LA-ISTW defected device are 0.26 eV, 0.28 eV, 0.24eV and 0.41eV, respectively. As shown in Figure 5, introducing LA-ISTW defects in AGNR channel near the drain contact (right side of the channel length) increases transport gap and consequently switching performance of transistor is improved. The observed transport gap isn't a band gap. Different reasons have been given for the transport gap formation in the graphene structures, such as Coulomb blockade effect in quantum dots [44], Anderson localization caused by edge irregularities [45], and a penetrance driven metal-insulator transition. Figure 5 also shows that T(E) has quantized in conventional structure. The quantization of T(E) shows carriers transmit by dissimilar separate modes. However it has not quantized in defected structures. This may be due to the asymmetry caused by the defects in these structures. For the conventional structure, the first flat surface in T(E) profiles extended to 0.3eV above and -0.4eV below the Fermi level. However, for the device with LA-ISTW defect near drain contact, the first flat surface of transmission is removed and one transmission valley is created nearly 0.21eV. This is due to the generation of strong carrier back-scattering as a result of that the quantum transport channel is completely stopped. In the absence of back-scattering effect, charge carriers can pass micrometer distances before trying a scattering happening [46]. When defect is located at the center or near the source, transmission T(E) significantly reduces and led to more reduction of ON current in transistor. The output characteristics of DG-AGNRFET in the presence of LA-ISTW defect in three different locations along the channel are all shown in Figure 6. The results indicate that adding the defects in the channel leading to decreasing the ON current. This decrement is minimum when defect is close to drain and is maximum when defect is in the middle of the channel.

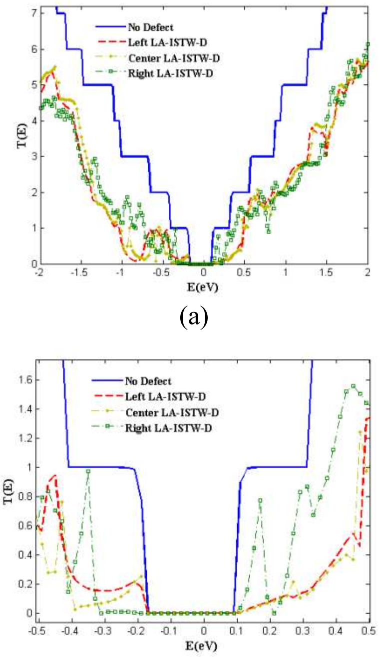

(a)

(b)

Figure 5: The transmission T(E) as a function of energy at various locations of LA-ISTW defect when the device is in the OFF state(defect density is 1.5%)(a)main plot and (b)a magnification view of the center side of the main plot.

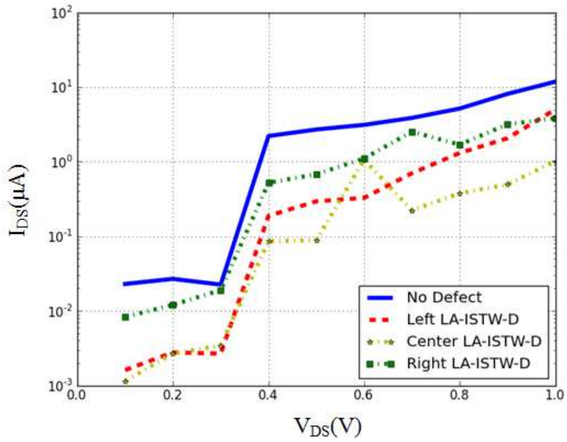

Figure 6: Drain current ID versus VDS characteristics for the defectless-DG-AGNRFET and defected-DG-AGNRFET (VGS = 0.5 V).

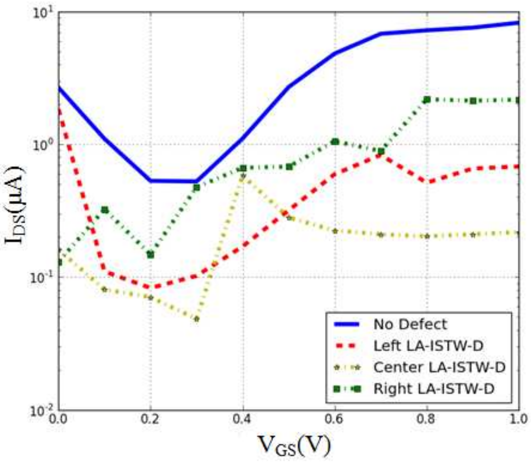

Figure 7: Drain current ID versus gate voltage VG characteristics for the conventional DG-AGNRFET and defected-DG-AGNRFET. The OFF and ON states respectively correspond to the gate voltages VG=0.0 and VG=0.5 V for the same drain voltage VD=0.5 V.

Figure 7 shows transfer characteristics of the DG-AGNRFET in the presence LA-ISTW defects. As shown in Figure 7; there is a significant ambipolar behavior in the vicinity of the OFF state leading to high leakage current in transistor. Presence of these defects in the center of the channel also reduces electrical current and increases the bandgap. Its high bandgap created in mid-channel leads to loss of controllability drain current by gate voltages, and consequently more fluctuations of ID-VGS characteristics. Adding such defects near the drain contact significantly reduce ambipolar conduction and consequently leakage current is also reduced. As a result, in this case, off current is 20 times smaller than that in the conventional structure and accordingly on/off current ratio increases and when defects are located near drain contact, its value is 4 times bigger than that in conventional structure. Therefore, the structure with defect added near the drain contact, has a higher on current and lower leakage current than the conventional structure. It confirms that adding LA-ISTW defect near drain contact makes transistors appropriate for logic applications. Although, increasing the defect densities near drain contact had no impact on bandgap (as was shown in Figure 4). So, the bandgap increasing due to the defects does not affected directly on electrical characteristics and the position and the density of these defects is also important.

The intrinsic voltage gain, AV=gm/gd, is an appropriate criteria for assessing analogue applications of such devices. In order to extract intrinsic voltage gain, parameters of transconductance (gm) and output conductance (gd) need to be considered. According to the results obtained from Figures 8 and 9, gm and gd both are reduced in structure with defect. Intrinsic voltage gain characteristic is also shown in Figure 10 as a function of VDS. As depicted in Figure 10, in some bias voltages such VDS=0.3V, AV from 0.27 in conventional structure increased to 6.5 for structure with defect in center and for VDS=0.8, AV from 0.18 in conventional structure increased to 1.83 for structure with defect in the right side of channel.

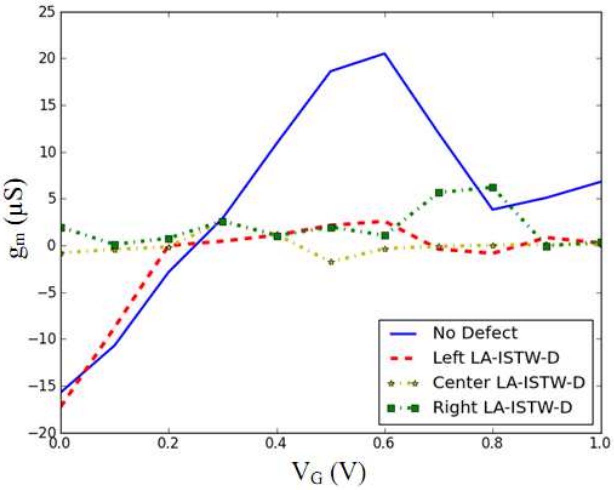

Figure 8: Variation of transconductance gm with VG at VDS = 0.5 V.

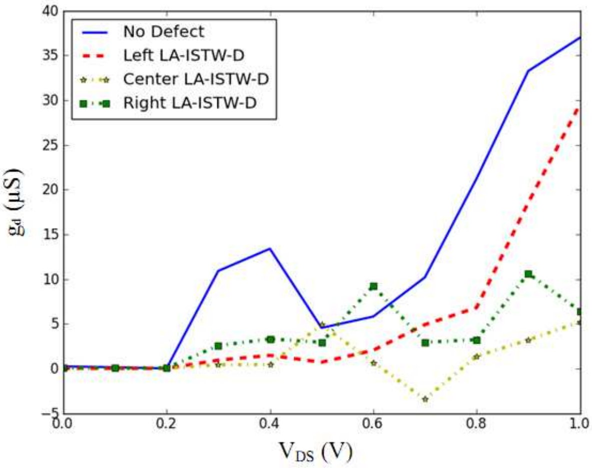

Figure 9: Variation of gd with drain voltage Vd at VGS = 0.5 V.

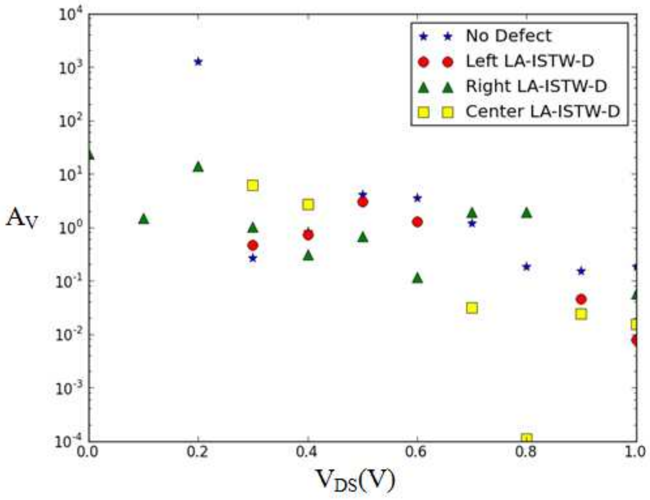

Figure 10: Variation of AV as a function of VDS for VG = 0.5 V.

Other appropriate criterion for evaluating analogue applications is the cut-off frequency fT which is computed as follows:

$$f_T = \frac{g_m}{2\pi C_g} \qquad (5)$$

Figure 11 indicates in low VGS's, fT from 2.5 in conventional structure increased to 6.5 for structure with defect in the center position.

Therefore, DG-AGNRFET with LA-ISTW defect in the appropriate bias and location along the channel can be useful for analogue applications

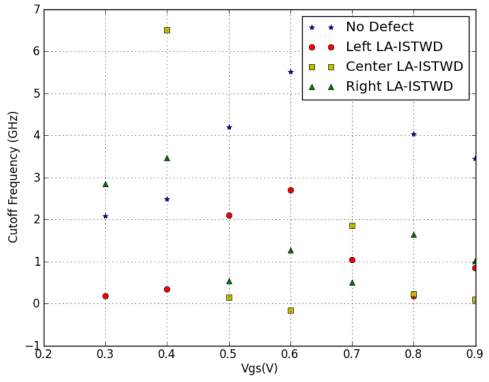

Figure 11: Variation of cut off frequency as a function of VGS .

.

4.Conclusion

In this paper, a novel investigation was proposed about the graphene nanoribbon transistor with linear arrangements of ISTW (LA-ISTW) defects. Based on the simulation results, using LA-ISTW defects with a proper defect density and in an appropriate location in channel length; defect engineering; led to bigger transport gap, bigger bandgap in the defective region, smaller off current and bigger on/off current ratio. Increase of on/off current ratio in graphene transistors caused by adding LA-ISTW defect along the channel, improves their performance for using in digital devices.

References

[1] S. Raghavan, I. Stolichnov, N. Setter, et al., "Long-term retention in organic ferroelectric-graphene memories," Appl. Phys. Lett. 100 (2) (2012): 023507.

[2] K. S. Novoselov, A. K. Geim, S. V. Morozov, D. Jiang, Y. Zhang, S. V. Dubonos, I. V. Grigorieva, A. A. Firsov, "Electric field effect in atomically thin carbon films," Science. 306 (2004): 666-669.

[3] A. A. Balandin, S. Ghosh, W. Bao, I. Calizo, D. Teweldebrhan, F. Miao, C. N. Lau, "Superior thermal conductivity of single-layer graphene," Nano Lett. 8(3) (2008): 902-907.

[4] Y. M. Lin, A. Valdes-Garcia, S. J. Han, D. B. Farmer, I. Meric, Y. Sun, Y. Wu, C. Dimitrakopoulos, A. Grill, P. Avouris, K.A. Jenkins, "Wafer-scale graphene integrated circuit," Science 332 (6035) (2011): 1294-1297.

[5] A. K. Geim, K. S. Novoselov, "The rise of graphene," Nat. Mater. 6 (2007): 183.

[6] T. Feng, D. Xie, H. Zhao, G. Li, J. Xu, T. Ren, H. Zhu, "Ambipolar/unipolar conversion in graphene transistors by surface doping," Appl. Phys. Lett. 103(19) (2013): 193502.

[7] F. Banhart, J. Kotakoski, A. V. Krasheninnikov," Structural defects in graphene," ACS Nano. 5(1) (2011): 26-41.

[8] I. Zsoldos, "Effect of topological defects on graphene geometry and stability," Nanotechnol. Sci. Appl. 3 (2010): 101.

[9] L. D. Carr, M. T. Lusk, "Defect engineering: Graphene gets designer defects," Nat. Nanotechnol. 5(5), (2010): 316-317.

[10] L. Vicarelli, S. J. Heerema, C. Dekker, H. W. Zandbergen, "Controlling defects in graphene for optimizing the electrical properties of graphene nanodevices," ACS Nano. 9(4) (2015): 3428-3435.

[11] H. Owlia, P. Keshavarzi, "Locally Defect-Engineered Graphene Nanoribbon Field-Effect Transistor," IEEE Trans. Electron Dev. 63(9) (2016): 3769-3775.

[12] H. Xu, D. Zhang, L. Chen, "Effect of defect on electronic properties of zigzag graphene nanoribbons," J. Cent. South Univ. 43(9) (2012): 3510-3516.

[13] K. L. Wong, M. A. S. Mahadzir, W. K. Chong, M. S. Rusli, C.S. Lim and M. L. P., Tan, "Graphene nanoribbon

simulator of vacancy defects on electronic structure," IJEEI. 6(3) (2018): 265-273.

[14] M. Poljak, E. B. Song, M. Wang, T. Suligoj, K. L. Wang, "Influence of edge defects, vacancies, and potential fluctuations on transport properties of extremely scaled graphene nanoribbons," IEEE. Trans. Electron Dev. 59(12) (2012): 3231-3238.

[15] I. Deretzis, G. Fiori, G. Iannaccone, G. Piccitto, A. La Magna, "Quantum transport modeling of defected graphene nanoribbons," Physica E: Low-dimensional Systems and Nanostructures Phys. E: Low-Dimens. Syst. Nanostruct. 44 (2012): 981-984.

[16] H. Zhang,G. Lee, K. Cho, "Thermal transport in graphene and effects of vacancy defects," Phys. Rev. B. 84(11) (2011): 115460.

[17] D. Orlikowski, M. Buongiorno Nardelli, J. Bernholc, C. Roland, "Ad-dimers on strained carbon nanotubes: A new route for quantum dot formation," Phys. Rev. Lett. 83(20) (1999): 4132.

[18] H. Zeng, J. Zhao, J. W. Wei, H. F. Hu, Effect of N doping and Stone-Wales defects on the electronic properties of graphene nanoribbons, Eur. Phys. J. B. 79(3) (2011): 335-340.

[19] A. Nazari, R. Faez, H. Shamloo," Improving ION/IOFF and sub-threshold swing in graphene nanoribbon field-effect transistors using single vacancy defects," Superlattices Microstruct. 86, (2015): 483-492.

[20] D.G. Kvashnin, L. A. Chernozatonskii, "Impact of symmetry in transport properties of graphene nanoribbons with defects," Appl. Phys. Lett. 105(8) (2014): 083115.

[21] J. Ma, D. Alfe, A. Michaelides, E. Wang, "Stone-Wales defects in graphene and other planar sp2-bonded materials," Phys. Rev. B. 80(3) (2009): 033407.

[22] S. Bhowmick, U. V. Waghmare, "Anisotropy of the Stone-Wales defect and warping of graphene nanoribbons: A first-principles analysis," Phys. Rev. B. 81(15) (2010): 155416.

[23] Y. Ren, K. Q. Chen, "Effects of symmetry and Stone–Wales defect on spin-dependent electronic transport in zigzag graphene nanoribbons," J. Appl. Phys. 107(4) (2010) 044514.

[24] J. Zhao, H. Zeng , B. Li, J. Wei, J. Liang, "Effects of stone-wales defect symmetry on the electronic structure and transport properties of narrow armchair graphene nanoribbon," J . Chem. Phys. 77 (2015): 8-13.

[25] M. T. Lusk, D. T. Wu, L. D Carr, "Graphene nanoengineering and the inverse Stone-Thrower-Wales defect," Phys. Rev. B. 81(15) (2010): 155444.

[26] M. T Lusk, L. D Carr, "Nanoengineering defect structures on graphene," Phys. Rev. Lett. 100 (17) (2008): 175503.

[27] A. P. Sgouros, G. Kalosakas, M. M. Sigalas, K. Papagelis, "Exotic carbon nanostructures obtained through controllable defect engineering," RSC Advances. 5(50) (2015): 39930-39937.

[28] S. Fotoohi, M. K. Moravvej-Farshi, R. Faez, "Electronic and transport properties of monolayer graphene defected by one and two carbon ad-dimers," Appl. Phys. A. 116(4) (2014): 2057-2063.

[29] S. Fotoohi, M. K. Moravvej-Farshi, R. Faez, "Role of 3D-paired pentagon–heptagon defects in electronic and transport properties of zigzag graphene nanoribbons," Appl. Phys. A. 116(1) (2014): 295-301.

[30] M. B. Nasrollahnejad, P. Keshavarzi, "Inverse Stone Thrower Wales defect and transport properties of 9AGNR Double-gate Graphene Nanoribbon FETs," J. Cent. South. Univ. 26(11) (2019): 2943-2952.

[31] L. Kou, C. Tang, W. Guo, C. Chen, "Tunable magnetism in strained graphene with topological line defect," ACS Nano. 5(2) (2011): 1012-1017.

[32] S. Okada, T. Kawai, K. Nakada, "Electronic structure of graphene with a topological line defect," *J. Phys. Soc. Jpn* .80(1) (2011): 013709.

[33] J. H. Chen, G. Autès, N. Alem, F. Gargiulo, A. Gautam, M. Linck, C. Kisielowski, O. V. Yazyev, S.G. Louie, A. Zettl, "Controlled growth of a line defect in graphene and implications for gate-tunable valley filtering," Phys. Rev. B. 89(12) (2014): 121407.

[34] J. Lahiri, Y. Lin, P. Bozkurt, I. I. Oleynik, M. Batzill, "An extended defect in graphene as a metallic wire," Nat. Nanotechnol. 5(5) (2010): 326 .

[35] M. H. Tajarrod, H. Rasooli Saghai, "High Ion/Ioff current ratio graphene field effect transistor: the role of line defect," Beilstein J. Nanotechnol. 6(1) (2015): 2062-2068.

[36] D. Gunlycke, C. T. White, "Graphene valley filter using a line defect," Phys. Rev. Lett. 106(13) (2011): 136806.

[37] D. A. Bahamon, A. L. C. Pereira, P. A. Schulz, "Third edge for a graphene nanoribbon: a tight-binding model calculation," Phys. Rev. B. 83(15) (2011):155436.

[38] H. Owlia, P. Keshavarzi, "Investigation of the novel attributes of a double-gate graphene nanoribbon FET with AlN high-κ dielectrics," Superlattices Microstruct. 75 (2014): 613-620.

[39] M. B. Nasrollahnejad, P. Keshavarzi, "Inverse Stone Throwers Wales defect and enhancing ION/IOFF ratio and subthreshold swing of GNR transistors," Eur. Phys. J. Appl. Phys. 86(2) (2019): 2.

[40] H Owlia, P Keshavarzi, M. B Nasrollahnejad, “Effects of Stone - Wales Defect Position in Graphene Nanoribbon Field - Effect Transistor”, J. Nano. Elec. Phys. 9(6) (2017): 06008.

[41] S. Datta, "Quantum Transport: Atom to Transistor" (Cambridge University Press, New York, 2005)

[42] F. Hao, D. Fang, Z. Xu, "Mechanical and thermal transport properties of graphene with defects," Appl. Phys. Lett. 99(4) (2011): 041901.

[43] M. Poljak, and T. Suligoj, "Quantum transport analysis of conductance variability in graphene nanoribbons with edge defects." IEEE Trans. Electron Dev. 63(2) (2015): 537-543.

[44] F. Sols, F. Guinea, A. H, Castro Neto, "Coulomb blockade in graphene nanoribbons," Phys. Rev. Lett. 99(16) (2007): 166803.

[45] D. Gunlycke, D. A. Areshkin, C. T. White, "Semiconducting graphene nanostrips with edge disorder," Appl. Phys. Lett. 90(14) (2007): 142104.

[46] J. H. Chen, C. Jang, S. D. Xiao, M. Ishigami, M. S. Fuhrer, "Intrinsic and extrinsic performance limits of graphene devices on SiO2," Nat. Nanotechnol. 3(4) (2008):206-209.